Effect of Hofmeister and Alkylcarboxylate Anionic Counterions on the Krafft Temperature and Melting Temperature of Cationic Gemini Surfactants

ARTICLE *in* LANGMUIR · JANUARY 2013

Impact Factor: 4.46 · DOI: 10.1021/la304341x · Source: PubMed

4 AUTHORS, INCLUDING:

Sabine Manet
Pierre and Marie Curie University - Paris 6
15 PUBLICATIONS **232** CITATIONS
SEE PROFILE

Yevgen (Eugen) A. Karpichev
Tallinn University of Technology
42 PUBLICATIONS **284** CITATIONS
SEE PROFILE

Reiko Oda
French National Centre for Scientific Resea…
74 PUBLICATIONS **2,713** CITATIONS
SEE PROFILE

Langmuir

The ACS Journal of Surfaces and Colloids

MARCH 19, 2013
VOLUME 29, NUMBER 11
pubs.acs.org/Langmuir

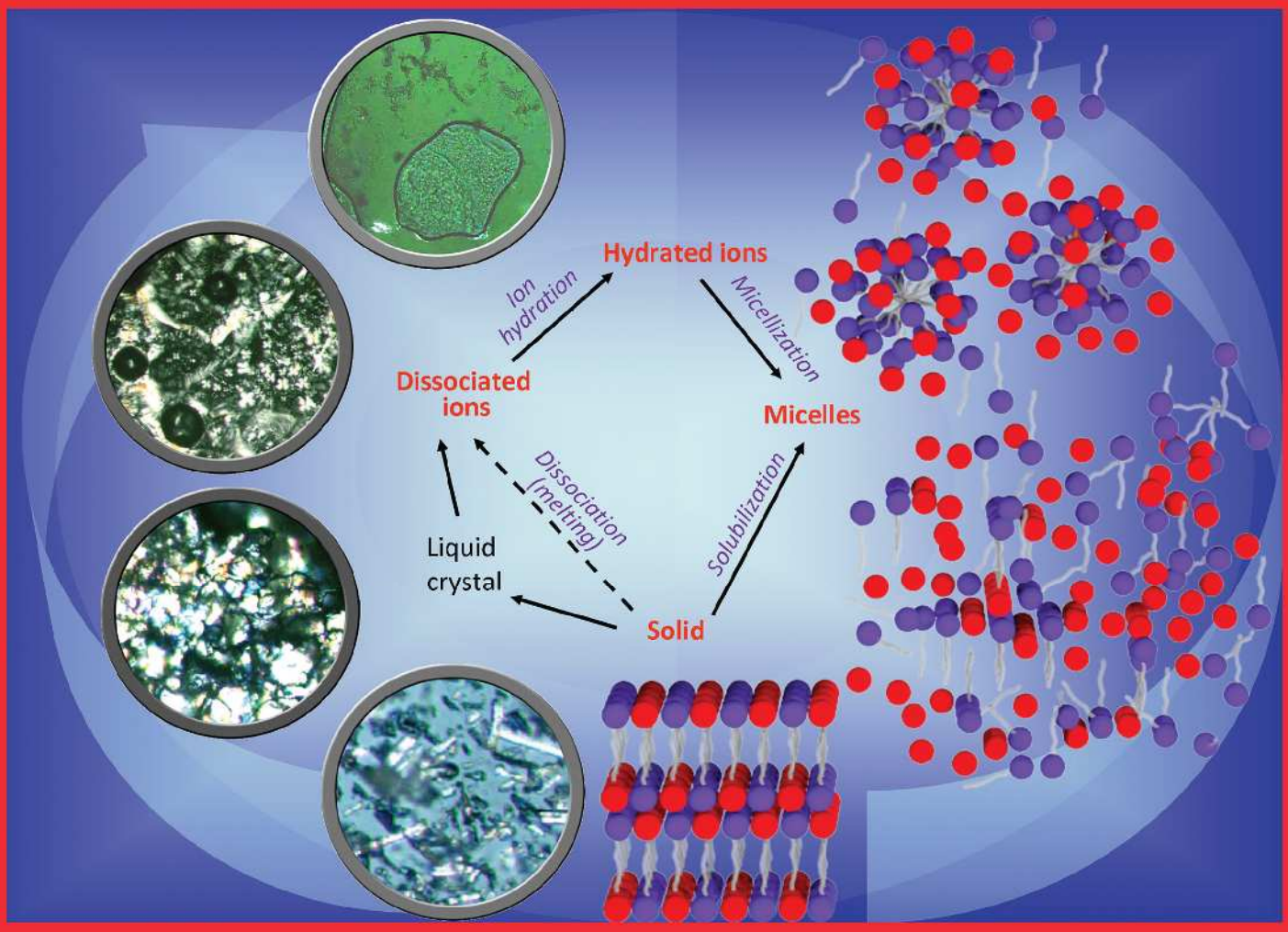

Subtle Balance between Ion Dissociation and Ion Hydration Dictates Solubilization of Charged Surfactants

(see p. 5A)

ACS Publications
MOST TRUSTED. MOST CITED. MOST READ.

www.acs.org

Langmuir

Editorial

pubs.acs.org/Langmuir

Biographical Sketches

Sabine Manet received her B.Sc. and M.Sc. from the Université Clermont-Ferrand II. She received her Ph.D. (physical chemistry) from Université Bordeaux I under the supervision of R. Oda, focusing on counterion effects on cationic surfactant assemblies. She was a postdoctoral fellow in the Laboratoire de Physique des Solides in the Université Paris Sud (M. Impéror), the Centre de Recherches sur les Macromolecules Végétales (CNRS, Grenoble) with L. Heux. Currently she works with L. Reven and M. Sutton at the Centre for Self-Assembled Chemical Structures at McGill University (Montreal).

Dmytro Dedovets received his M.Sc. from Donetsk National Technical University (Donetsk, Ukraine), Department of Ecology and Chemical Technology by Specialty: Chemical Technology of Fuel and Carbon Materials. Since December 2010, he has been a Ph.D. student at University Bordeaux I (Bordeaux, France), Department of Chemical Science (physical chemistry of condensed matter); his project is titled "Functional Hybrid Organic−Inorganic Nanohelices: Studies of the Exalted Phonomena at Nanometric Scales".

Yevgen Karpichev received his Ph.D. in 2002 from University of Donetsk (Ukraine). After postdoctoral work at Dalhousie Univesity, he joined Dr. Oda's group as a postdoctoral research associate to study counterion effects on the micellar properties of gemini surfactants. Since 2010, he has been working as senior research fellow at L. M. Litvinenko Institute of Physical Organic Chemistry and Coal Chemistry, NAS of Ukraine. His interests include the development of functionalized surfactants, micellar catalysis, and organic reactivity in organized molecular systems.

Reiko Oda obtained her B.Sc. in physics at the University of Tokyo and her Ph.D. in physics at the Massachusetts Institute of Technology (D. Litster) for the project "X-Ray Diffraction Study of Three-Component Lamellar Phases". She was a postdoctoral fellow at the University Louis Pasteur (Strasbourg, S. J. Candau) working on the rheological properties of wormlike micelles of cationic gemini surfactants. She joined the IECB in 1998 as a group leader and created the group "Morphologies, Dynamics and Functions of Assemblies of Amphiphiles". She is interested in understanding the mechanism of formation of molecular assemblies in order to design and build new nanometric molecular assembly systems of amphiphilic molecules, the morphologies and functions of which can be finely tuned.

Published: March 19, 2013

dx.doi.org/10.1021/la400344z | *Langmuir* 2013, 29, 3511−3511

Langmuir

Invited Feature Article

pubs.acs.org/Langmuir

Effect of Hofmeister and Alkylcarboxylate Anionic Counterions on the Krafft Temperature and Melting Temperature of Cationic Gemini Surfactants

Sabine Manet,[†] Yevgen Karpichev,[†,‡] Dmytro Dedovets,[†] and Reiko Oda*[,†]

[†]UMR 5248 CBMN, CNRS-Université de Bordeaux, Institut Européen de Chimie et Biologie, 2 rue Robert Escarpit, F-33607 Pessac, France

[‡]Litvinenko Institute, National Academy of Sciences of Ukrain, 70, R. Luxemburg Str., 83114, Donetsk, Ukraine

Supporting Information

ABSTRACT: The effect of counterions was investigated to probe the principal ionic effects on the solubility in water and melting behavior of cationic gemini surfactants. We focused on two types of counterions: (1) small inorganic counterions that are typically taken from the Hofmeister series were studied to focus on the effect of ion type and (2) *n*-alkylcarboxylate counterions were studied to focus on the effect of the hydrophobicity of counterions. The Krafft temperature (T_k) and melting temperature (T_m) were obtained by conductivity measurements, calorimetric measurements, and optical microscopy observation. The results clearly indicate that T_k, which represents the solubility of surfactants, is not determined by a single parameter of ions such as the hydration free energy, as is too often assumed, but rather by the combined effects between the hydrophobicity of anions associated with other effects such as the polarizability, dehydrated ion size, and ionic morphology. In parallel, our observation demonstrated that all of the surfactants showed a transition from a crystalline phase to a thermotropic liquid-crystalline phase at around ca. 70 °C, which transformed to an isotropic liquid phase at around ca. 150 °C, and that the transition temperatures depended strongly on the counterion type. The counterion effects on the solubilization and melting behaviors were then compared with micellization properties that have been reported previously. These results provide new insight into understanding the effect of ions on the delicate balance of forces controlling the solution properties and aggregate morphology of charged amphiphilic molecules. Specifically, the solubilization properties of these cationic surfactants with various counterions were determined mainly by the subtle interplay between the hydration of counterions and the dissociation energies (stability of crystallinity) of the ion pair.

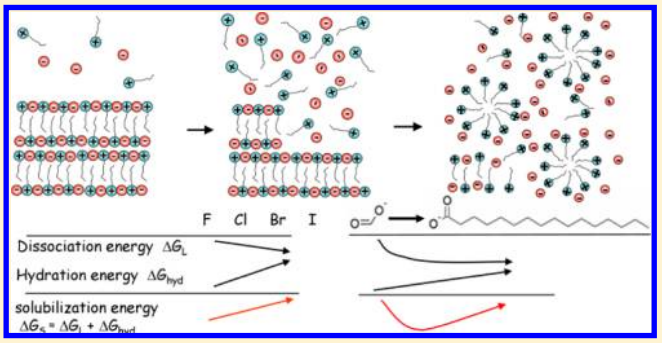

INTRODUCTION

Since the first explicit account of ion specificity by Hofmeister on the salt effect on protein solutions in the late nineteenth century, the ion effect has been widely reviewed both experimentally and theoretically.[1−7] It would be impossible to draw up an exhaustive list of phenomena affected by ionic effects.[8] In biological systems, for instance, the water absorbance of wool fibers and the growth of a bacterium are related to ion specificity.[7] A number of reports have dwelled on the ion dependence of the surface tension of aqueous electrolyte solution by molecular simulation studies.[9−11] However, classical theories based on van der Waals interactions and the electrical double layer still fail to explain a fundamental observation. A number of semiempirical models have been proposed in which the degree of organization of water molecules surrounding the ion is crucial, where kosmotropic ions exhibit strong interactions with water and chaotropic ions are less hydrated and thus less effective in organizing the surrounding water molecules. Many attempts have been proposed to correlate Hofmeister effects with other properties of ions. For example, the free energy and entropy of hydration, free energy of transfer from the aqueous to the organic phase, hydrated ionic radii, partial molar volume, and polarizability closely correlate with the Hofmeister hierarchy of ions.[12−15]

Amphiphilic molecules in water show various intermediate states or mesophases between precipitates and the molecular solution. Indeed, their ambivalent nature can lead to the formation of self-assemblies with extremely rich polymorphism. At very low concentration, the phase diagram that describes the thermodynamical state of a given amphiphilic molecule can be characterized by two principal parameters, the critical micellar concentration (cmc) and the Krafft temperature (T_k). T_k is the temperature above which an ionic surfactant becomes soluble and forms micelles. Below T_k, the concentration of monomeric

Received: November 1, 2012
Revised: January 23, 2013

   dx.doi.org/10.1021/la304341x | *Langmuir* XXXX, XXX, XXX−XXX

surfactant in solution is limited by its weak solubility determined by the balance of the lattice energy (or dissociation energy) of crystals/precipitates and the hydration energy of the ionic species. At T_k, this concentration reaches the cmc, the thermodynamic balance is therefore shifted toward micelle formation, and the solubility of the surfactant increases suddenly. Thus, T_k depends not only on the solubility of the monomers but also on the balance of (1) the stability of the solid state of the surfactant (lattice energy), (2) the hydration energy of ions, and (3) the free energy of micelle formation. Obviously, both the cmc and T_k are strongly influenced not only by the nature of the counterions[8,16] but also by the degree of ionization of the micelles, the aggregation number,[17] the amount of water or counterions in the interfacial region,[18] and the morphology of self-assembly,[19−29] which all depend on the nature of the counterions as investigated experimentally[30,31] and by molecular simulation studies.[9−11,32]

Recently, we reported the counterion effect on the micellization behavior of *n*-2-*n* gemini surfactants (cmc, degree of ionization, and aggregation number, respectively) using conductivity, fluorescence, and UV−vis measurements.[33] Gemini surfactants are a group of amphiphilic molecules that have generated much interest for more than 20 years owing to their unique aggregation behavior.[34−39] In spite of the structural diversity of gemini surfactants in the literature, only a few studies have focused on the counteranion effect on the properties of bisquaternary ammonium-type cationic gemini *n*-*s*-*n* surfactants with counterions other than bromide and chloride.[40−47]

In that study, we reported[33] the effect of 30 different counterions classified into four principal groups: (1) small counterions, which are principally ions taken from the Hofmeister series, (2) aliphatic carboxylate counterions, where the hydrophobicity of the anion can be tailored by modifying the alkyl group while keeping the same ionic nature, (3) aromatic carboxylate counterions, where the effect of substitution can be examined, and (4) those counterions that do not belong to the first three families but allow comparisons based on particular properties (i.e., "orphan" counterions)

The results globally confirmed the tendencies expected from the hydrophobicity/hydrophilicity of anions that promote or inhibit micellization (i.e., the more hydrophobic the counterions, the smaller the cmc's). The small anions generally show a correlation with the Hofmeister series, known to be related to the polarizability of ions. Chaotropic anions are highly polarizable and are far more effective at ion-pair formation promoting the micellization process and micellar growth of ionic surfactants in comparison to kosmotropic ions. However, for polyatomic ions, the effect of ion properties on the aggregation behavior of the amphiphiles can be largely perturbed by steric effects or intermolecular/intramolecular interactions via hydrogen bonds and the hydrophobic effect. Also, the additional entropic effects associated with the liberation of water molecules during micellization are clearly observed.

In the present study, the effects of small counterions and aliphatic carboxylate counterions X^- on T_k and the melting temperature (T_m) of cationic gemini surfactants ethanediyl-α,ω-bis(dimethylalkylammonium (*n*-2-*n*) are reported for three different chain lengths, *n* (Chart 1). The results clearly demonstrated that the solubility of the surfactants as observed by the Krafft temperature are determined by the balance of the lattice energy of crystals/precipitates closely linked to the melting temperatures and the hydration energy of the ionic species. Although the hydration energy of the ionic species is strongly related to the nature of the ions, such as their polarizabilities and hydration energies,[20] the melting temperature seems to be strongly linked to the parameters that influence the packing of solids, such as the ion size and the presence of hydrocarbon chains. Interestingly, these two effects (ion size/polarizability and hydration energy) may lead to opposite trends (e.g., for the carboxylate counterions, the melting temperature decreases between $n = 1-10$ and flattens out for $n = 12-16$ whereas the hydrophobicity increases monotonously). The observed T_k shows a combined effect going through a minimum. Closer examination revealed a complex melting procedure for some of the gemini surfactants. All of them go through at least two steps (crystal to liquid crystal and then to the liquid phase), as previously reported for similar gemini surfactants.[48−50]

Herein, we will discuss that the solubilization is a complex phenomenon where the melting, ion hydration, and micellization (cmc) processes play important roles.

Chart 1. Cationic Gemini Surfactant *n*-2-*n* with Counterion X, Denoted as *n*-2-*n* X or *n*X, along with the Naming System Adopted

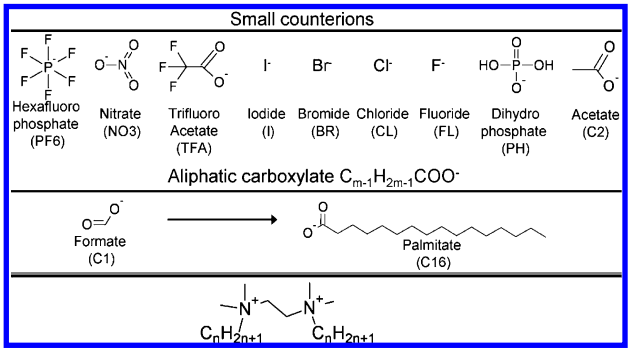

EXPERIMENTAL PART

Synthesis. The *n*-2-*n* surfactants with various counterions were synthesized as previously reported.[33]

Krafft Temperatures (T_k). The Krafft temperature measurements were performed with 5 mL of 3 mM surfactant solutions in ultrapure water (ELGA purelab ultra 18.2 MΩ·cm). The Krafft temperature is the temperature at which the hydrated surfactant dissolves in water; therefore, all of the samples were first dissolved in water by warming and were then plunged into liquid nitrogen. This quick cooling allowed us to obtain the precipitation of a very fine, hydrated powder before the experiment. The conductivity was measured as the temperature was increased until above the clarification of the solution. The Krafft temperature was taken as the temperature at which the conductivity versus temperature plot showed a break.

Melting Temperature (T_m). The melting temperature was measured with an optical microscope coupled to a Mettler Toledo (Columbus, OH, USA) FP900 thermosystem. A small amount of the sample powder was put between a glass slide and a glass coverslip, placed on an FP82HT hot stage, and heated at a rate of 0.5 to 1 °C/min. The transformation of the sample was followed using a Nikon Eclipse Physio Station E600FN optical microscope.

Differential Scanning Calorimetry (DSC). DSC experiments were performed with a DSC Q100 V9.9 Build 303 instrument (TA Instruments). Every sample was scanned at least three times at a scanning rate of between 5 and 10 °C/min.

dx.doi.org/10.1021/la304341x | *Langmuir* XXXX, XXX, XXX−XXX

RESULTS

Krafft Temperature. *Small Counterions.* Figure 1 shows how the Krafft temperatures of gemini *n*-2-*n* vary as a function

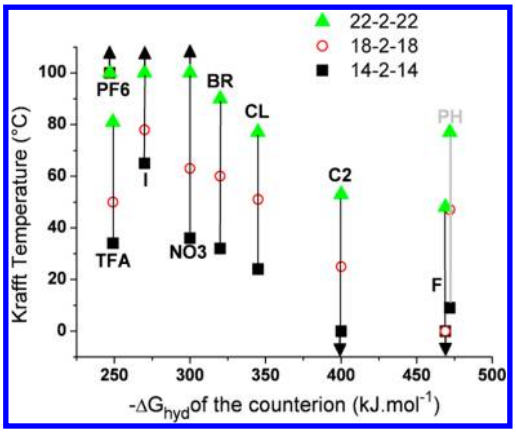

Figure 1. Krafft temperature of gemini 14-2-14, 18-2-18, and 22-2-22 with small counterions as a function of the free energy of hydration ($-\Delta G_{hyd}$). Arrows indicate that the Krafft temperature is above 100 °C or below 4 °C.

of the free energy of hydration, ΔG_{hyd}, of small counterions for n = 14, 18, and 22. The observed trend globally confirmed that the higher the $-\Delta G_{hyd}$ values (i.e., the higher the energy gain upon hydration of the ions), the lower the T_k values of the Gemini surfactants. As expected, T_k increases with increasing hydrophobic chain length (T_k (n = 14) < T_k (n = 18) < T_k (n = 22)). For example 18-2-18 having iodide (I^-) as the counterion has a T_k value of 80 °C whereas when the counterion is fluoride (F^-) the molecule is still soluble at 4 °C. This tendency is in good agreement with what we have observed previously regarding the relationship between the hydrophilicity of the counterion and the micellization process on the cmc.[33]

Nevertheless, there are some ions, such as trifluoroacetate (TFA) and dihydrophosphate (PH), that do not exactly follow this trend in hydrophobicity: gemini TFA ($-\Delta G_{hyd}$ = 251 kJ/mol) has lower T_k values than what is expected from the very high hydrophobicity of TFA. Inversely, gemini PH has higher T_k values than gemini F in spite of the similar free energies of hydration, ΔG_{hyd}, of F and PH.

n-Alkylcarboxylate Counterions. The T_k values obtained for gemini surfactants (n = 14, 18, and 22) with aliphatic carboxylate counterions (m = 1−16) are presented in Figure 2 along with the log P of ion transfer for the system water−nitrobenzene for an alkylcarboxylate with various hydrophobic chain lengths taken from ref 51. Interestingly, the evolution of the T_k of 18-2-18 with m shows a minimum at m = 4, whereas the minimum is shifted to m = 6−8 for 22-2-22. For 14-2-14, they are all soluble with $C_mH_{2m+1}COO^-$ counterions at 3 mM in water at 4 °C for m < 8. Above m = 8, the T_k values increase monotonously. As is well known, the log P, which represents the hydrophobicity of the ions, increases monotonously with the hydrocarbon chain length. The presence of the minima for T_k values indicates that the T_k does not simply follow the hydrophilicity/hydrophobicity trend.

Melting Temperature. We also investigated the melting process of the dry powder with an optical microscope. Figure 3 shows the optical microscope images of various samples in three phases: (1) a crystalline phase, (2) different types of liquid-crystalline phases, and (3) an isotropic liquid phase.

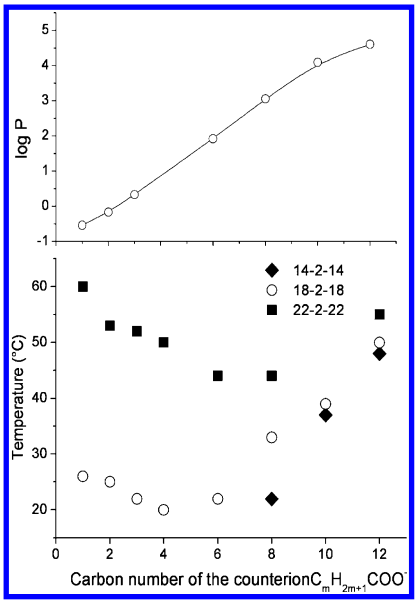

Figure 2. (Top) log P energy of ion transfer for the system water−nitrobenzene system for an alkylcarboxylate with various hydrophobic chain lengths from ref 51. (Bottom) Krafft temperature of geminis 14-2-14, 18-2-18, and 22-2-22 with n-alkylcarboxylate counterions $C_mH_{2m+1}COO^-$ as a function of the length m.

It was clearly observed that melting followed different processes with several types of transitions depending on the counterions.

Most of the samples showed a crystal to liquid crystal transition first upon heating. The nature of the liquid-crystalline (LC) phase depends strongly on the counterions. We have identified three different types of LC phases as described below: Xa, Xb, and SmA. For the majority of cases, the crystalline birefringent powder (CR) turns into a viscous, very birefringent LC phase (Xb) upon heating. Then at a higher temperature, a transition to another liquid-crystalline phase with a much lower viscosity with focal conic texture and a liquidlike boundary (droplet) was observed. This phase (SmA) presents smectic A-type texture. Finally, at a higher temperature the transition to the isotropic liquid phase (I) was observed. In the case of 14-2-14 PH and 14-2-14 Palm, there was no transition from the pastelike mesophase with high viscosity (Xb) toward a more fluidlike SmA with a smooth meniscus (Supporting Information), and the Xb-type viscous mesophase either transformed directly to the isotropic liquid (14-2-14 Palm) or the sample underwent degradation (14-2-14 PH). For other samples such as 14-2-14 BR and 14-2-14 CL, another type of transition was observed where the crystal structure with strong birefringence transforms to another crystalline-like structure with much weaker birefringence (Xa).

In Figure 4, the transition temperatures during the melting of the gemini surfactants are presented. The thermotropic behavior of the gemini surfactant is strongly influenced by the counterions. Globally, there are large differences in the crystal to liquid-crystalline transition temperatures between chaotropic and kosmotropic counterions: hydrophobic counterions such as I^-, NO_3^-, TFA, and Br^- show CR to Xa, Xb, or SmA above 100 °C. Counterions such as F^-, acetate, and Cl^- show a transition to the LC (Xb or SmA) phase at lower temperatures (except for PH). They also show an important temperature range of the SmA phase as clearly observed by polarized light microscopy. The melting transitions to the

dx.doi.org/10.1021/la304341x | Langmuir XXXX, XXX, XXX−XXX

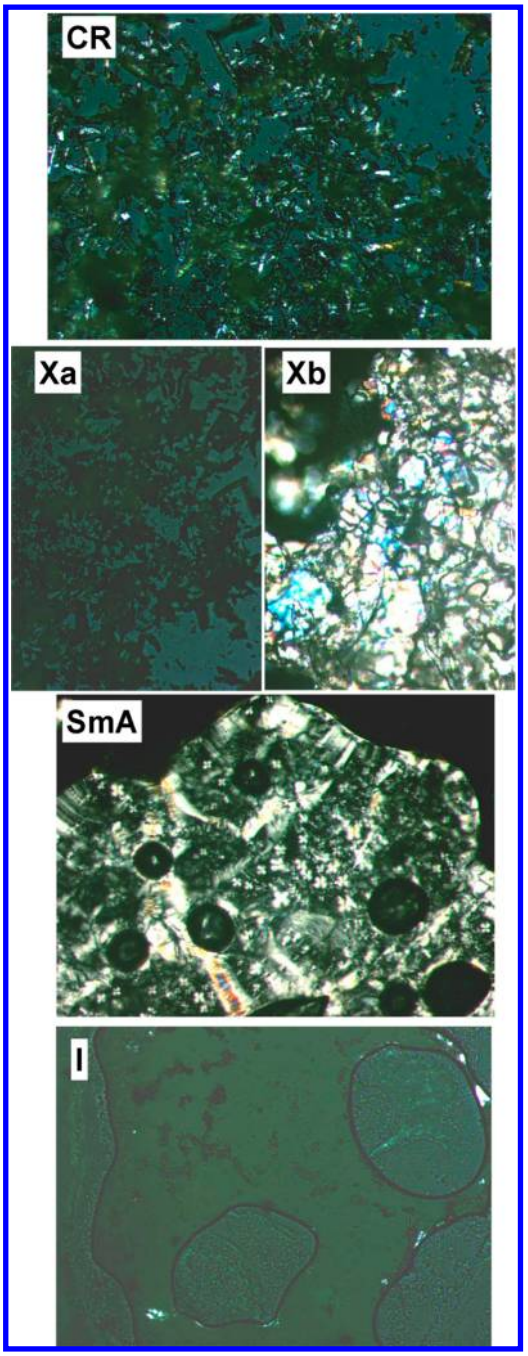

Figure 3. Various phases observed with a polarized optical microscope. As noted in the text, different samples show different transitions (e.g. 14-2-14 I shows a CR to Xa to I transition and 14-2-14 CL shows a CR to Xb to SmA to I transition).

isotropic liquid phase (LC to I) do not vary much with the nature of the counterions. They all vary between 155 and 175 °C except for PH, NO_3^-, and F^- that degrade at 190, 180, and 165 °C, respectively.

Interestingly, for the halide counterions, the LC to I transition of the surfactant decreases slightly with increasing ionic radius of the counterion: 175 °C for I^-, 180 °C for Br^-, and 185 °C for Cl^-, except for F^-, which degraded at ca. 165 °C. This is in agreement with what we have reported in detail previously[52] (i.e., free energies for the formation of ion pairs of bolaform 1-*n*-1 X in the gas phase as calculated with DFT decrease with increasing ionic radius (X = F^- −185.9, Cl^- −158.0, Br^- −150.8, and I^- −142.6 kcal mol^{-1})). Also, the comparison between the crystal structures of 14-2-14 I and 14-2-14 BR clearly show that the distance between I^- and N^+ is about 2 to 3 Å longer than the distance between Br− and N^+. The fact that 14-2-14 F has a low T_m is due to its high reactivity.[52] However, the CR to LC phase transition increases with increasing ionic radius: 37 °C for 14-2-14 F, 55 °C for 14-2-14 CL, 100 °C for 14-2-14 BR, and 105 °C for 14-2-14 I. As a result, the more hydrophobic the counterions, the smaller the temperature ranges of the LC phases for the halide series. The very high transition temperature of 14-2-14 PH is very surprising. Indeed, their crystalline structure is very stable, followed by stable liquid-crystalline phases that directly undergo degradation without reaching the real melting point (the melt liquid simultaneously becomes yellow-brown). This unusual behavior of PH ions will be discussed later.

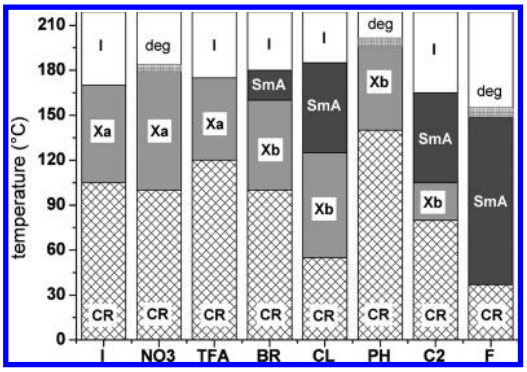

Figure 4. Phase-transition temperatures between various phases (I, Xa, Xb, SmA, and CR) for 14-2-14 with small counterions are shown with the counterions in the same order as presented in Figure 1. deg represents the degradation of the samples.

The thermotropic behaviors of the gemini surfactants with alkylcarboxylates are summarized in Figure 5. In this case, both the melting temperature LC to I and the C to LC transitions vary significantly with the carboxylate hydrocarbon chain length. For most of the samples except for palmitate, the CR phase shows a transition to Xb, then to SmA, and then to the I phase. The CR-to-Xb transition temperature decreases with *m* until it reaches a minimum at *m* = 6 and then increases again. For the Xb to SmA and SmA to I transitions, the transition temperatures show a maximum at *m* = 3 followed by a

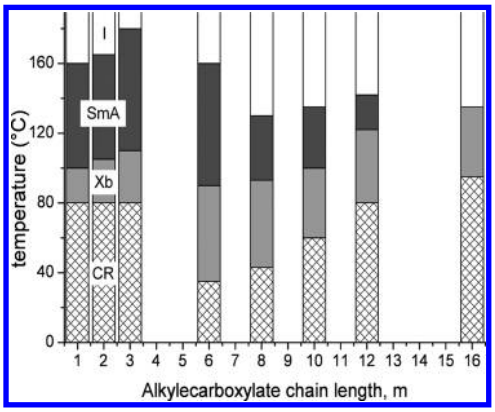

Figure 5. Phase-transition temperatures between various phases for 14-2-14 are shown with alkylcarboxylate counterions as a function of chain length *m*.

dx.doi.org/10.1021/la304341x | *Langmuir* XXXX, XXX, XXX−XXX

minimum at $m = 6-8$. The temperature range where the SmA phase is observed is much more pronounced for short chains and therefore for more hydrophilic gemini surfactants, in agreement with what was observed for small counterions shown in Figure 4.

The phase transition was also monitored with DSC measurements. Interestingly, we could observe that, in general, when the CR phase transforms to the Xa or Xb phase and directly to the I phase, the spectra are quite straightforward as shown in Figure 6 (14-2-14 I), with an important main peak

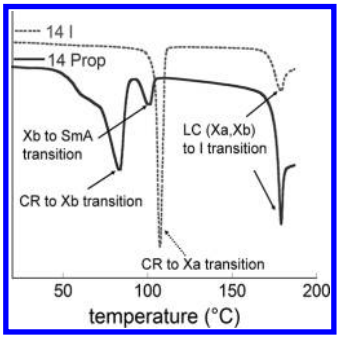

Figure 6. Typical DSC peaks for the CR-Xa-I transition (14-2-14 I) compared to the CR-Xb-SmA-I transition (14-2-14 Prop).

showing the melting from CR to LC(Xa) and a smaller peak showing the LC(Xa) to I transition. However, the sequential transition from CR to LC(Xb) and then from LC(Xb) to SmA is often characterized by broader and more complex peaks, followed by the similar smaller peak for the LC to I transition in Figure 6 (14-2-14 Prop). For those systems that showed browning (degradation) during heating (F−PH and NO_3^-) with microscopic observation as mentioned above, sample degradation was confirmed by the absence of peaks upon reheating a cooled sample after a day at room temperature.

DISCUSSION

Process of Solubilization. Let us examine the process of solubilization at the Krafft temperature when the temperature of an ionic surfactant suspension in water is increased at a given concentration beyond the cmc. When the temperature increases, the solubilized surfactant monomer concentration in equilibrium with the solid increases until it reaches the cmc of the surfactant. At this moment, the solubility increases tremendously and the solid suspension disappears to form a micellar solution.

For a gemini $AX_{|(iz_s)/(z_c)|}$ where z_s and i are the charge and the number of surfactant polar heads, respectively, j is the number of alkyl chains, and z_c is the valence of the counterion X, this process can be seen as the result of three steps, illustrated in Figure 7: (1) dissociation: $AX_{|(iz_s)/(z_c)|} \rightarrow A_j^{iz_s} + X^{z_c}$; (2) hydration of ions: $A_j^{iz_s} + X^{z_c} \rightarrow A_j^{iz_s}(aq) + X^{z_c}(aq)$; and (3) micellization: $A_j^{iz_s}(aq) + X^{z_c}(aq) \rightarrow A_{j,N}^{Niz_s+pz_c}$

The lattice energy measures the amount of energy required to separate one mole of an ionic compound completely into its ions in the gaseous phase. Although beyond the melting of an ionic compound that we measure from the solid state the ions are not completely separated from each other, melting points are indicative of lattice energy, and a compound with higher lattice energy would have a higher melting point.[53] More symmetric molecules will have higher melting points because they pack more efficiently and thus have higher lattice energies.

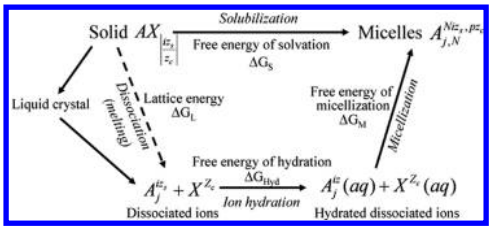

Figure 7. Three steps in the dissolution of an ionic surfactant at T_k: dissociation, hydration, and micellization.

The contribution of the lattice energy, ΔG_L, is positive, whereas the solvation process as described with the free energy of hydration, ΔG_{hyd}, of the species and the free energy of micellization is negative. As we have previously shown,[33] the absolute values of ΔG_{hyd} are about 10 times higher than that of the free energy of micellization, ΔG_M. Therefore, micellization is not the primary process that determines T_k, even if the influence of hydrophilicity is important in both cases. Along with the free energy of hydration of the ions, the stability of the solid state is the second key parameter of the solubilization process.

Thermotropic Properties. The analysis of the transitions that occur below the T_m of 14-2-14-type gemini surfactants provides insight into the counterion influence on the solid-state transformations. A low-viscosity mesophase formed by a majority of gemini surfactants studied (Figures 4 and 5) is a smectic A-type mesophase. Indeed, because of a combination of repulsive/attractive electrostatic forces between cations and anions and van der Waals hydrophobic interactions between alkyl chains, a smectic-type molecular arrangement with a layered structure is usually found in ionic liquid crystals formed by amphiphiles.[54,55] In SmA, the molecules are aligned perpendicular to the layers, with no long-range crystalline order within a layer, and the observed optical properties (Figure 3) are caused by the distortions of these layers.

The Xb mesophase (Figure 3) has a higher viscosity and always precedes, when it appears, the formation of SmA (except for 14-2-14 PH, which degrades before reaching its real melting temperature, and 14-2-14 Palm). Therefore, it can also be characterized as another smectic phase with a higher crystallinity. Indeed, a number of different classes of smectics have been recognized, and as a rule, the lower-temperature phases have a greater degree of crystalline order,[56] such as the T-type mesophase with tetragonal symmetry previously reported by Alami et al.[57] and later found for different liquid-crystalline systems.[58] For example, for a series of *n*-alkylpyrrolidinium salts, a smectic T arrangement characterized by tetragonal layes separated by hydrophobic alkyl chains has been reported to transform to a SmA mesophase.[59]

As for Xa (with a nonbirefringent crystalline-like structure), it has been reported that the nonbirefringent phase is also a mesophase, as observed by DSC and optical microscopy to become a birefringent viscous phase with the application of gentle pressure.[48] It is interesting that for the systems reported in this study the Xa phase was observed only within the "small" anion series for the most hydrophobic counterions, namely, TFA, I^-, Br^-, and NO_3^-. A similar situation has been reported for gemini surfactants with rigid piperazinium[60] and DABCO[61] spacer groups. For the two types of gemini surfactants with these rigid spacers, smectic T-phase formation, both birefringent or nonbirefringent, was reported.

dx.doi.org/10.1021/la304341x | Langmuir XXXX, XXX, XXX−XXX

Small Counterions. To understand the factors governing the transformations during the melting of 14-2-14 gemini surfactants of the "small" anion series, we analyzed the role of the dehydrated ion radius of the counterion in the temperature range of the LC. In Figure 8, the temperature of the first phase

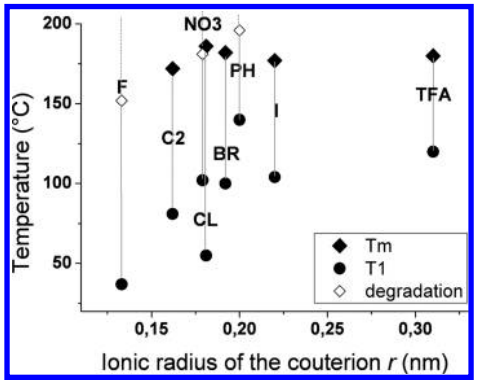

Figure 8. First phase-transition temperatures (T1) CR to LC (●), melting temperatures (T_m) (♦), and degradation temperature (◊) of 14-2-14 with small counterions plotted as a function of the dehydrated ion radii.

transition, CR to LC (T1), as well as the melting temperature (LC to I) is plotted as a function of the counterion radius. For the CR to LC transition temperature, the general trend clearly demonstrates that ions with large ionic radii (more polarizable) are characterized by a high transition temperature to the mesophase compared to that of smaller anions.

The LC to I transition temperature does not follow the same tendency as the CR to LC transition. Except for acetate (and F^-, NO_3^-, and PH, which all show degradation), larger ions tend to show lower LC to I transition temperatures (T_m): $I^- \approx$ TFA < Br^- < Cl^-. As discussed above, this is probably because smaller (less polarizable) anions have stronger cation–anion interactions in crystals. This suggestion is supported by several observations of the influence of the halide counterion on the temperature range of the surfactant mesophase where counterions increase the stability of the smectic LC phase in the order Cl^- > Br^- > I^-.[62−64] Although halides and tetrahedral anions (e.g., PH) are or are close to spherically symmetric, other polyatomic anions are nonspherical and cannot be assigned a unique radius. Therefore, only their apparent radii can be calculated from the lattice energy of the compounds containing these corresponding anions.[65,66]

Special attention should be paid to PH and TFA, which show particularly high (PH) and low (TFA) transition temperatures for both CR to LC and LC to I. Such a strong stability of 14-2-14 PH may be connected to the capability of PH to form hydrogen bonds. It is well known[67−69] that in the dihydrophosphate crystals the tetrahedral PO_4 units are linked by O···H···O hydrogen bonds and that the structure is stabilized by ionic cation–anion interactions. These bonds can increase the energy of mesophase formation, cause higher T1 values, and prevent the appearance of an SmA mesophase, even at temperatures close to the melting temperature.

As we have reported previously,[33] the cmc's of 14-2-14 gemini surfactants with small counterions are plotted in Figure 9 as a function of the hydration energy of the counterion. The more hydrophobic anions, namely, TFA, I^-, Br^-, and NO_3^-, with low $-\Delta G_{hyd}$ values have similarly low cmc values whereas gemini surfactants having anions with higher $-\Delta G_{hyd}$ values

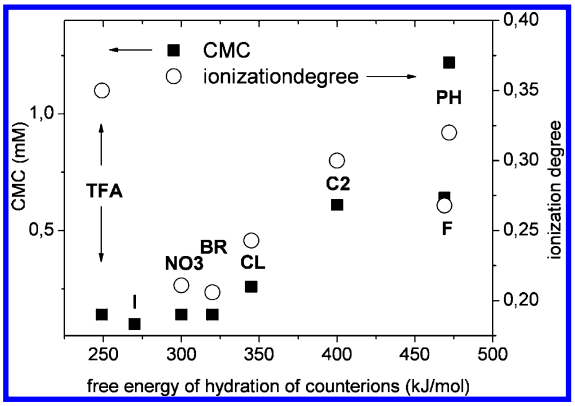

Figure 9. Critical micelle concentrations and degrees of ionization of 14-2-14 with small counterions as a function of the free hydration energy of the counterion.

have higher cmc values. It is interesting to compare 14-2-14 F and 14-2-14 PH. F and PH are characterized by almost the same value of the free hydration energy whereas their cmc values (0.64 and 1.28 mM, respectively) and free energies of micellization (20.58 and 17.87 kJ·mol^{-1}, respectively) are very different. As mentioned in previous work, the high cmc for 14-2-14 PH is probably due to the high polarizability and small number of PH ions of hydration.[33]

The abnormally high T_k of gemini PH as shown in Figure 1, in spite of the strong hydrophilicity of PH (it is more hydrophilic than C2 and has a similar hydrophilicity to that of F), can then be explained as a combined effect of the high lattice energy (T_m) and the high cmc (low free energy of micellization), supporting the scheme of the overall solubilization process (Figure 7). In other words, the solubilization of the small counterion is a result of the interplay of the three processes: dissociation, hydration, and micellization.

Gemini TFA, however, has a lower T1 value than expected from its ionic radius (Figure 8). This may be due to its weaker affinity for the hydrophobic hydrocarbon chains of the gemini surfactant because of the fluorine atoms, which leads to low crystal stability. This is also confirmed by the high degree of ionization as seen in Figure 9. However, its T_m is higher than predicted from the common trend, so crystalline-like mesophase type Xa is stabilized over a relatively wide temperature range. The solubilization behavior (T_k) of gemini TFA is also surprising. In spite of its large ionic radius, high polarizability, and low ΔG_{hydr}, the T_k values of gemini TFA are small compared to those of gemini surfactants with counterions of similar hydrophobicities. Probably the same reasons for the origin of low T1 (weak affinity of gemini and TFA and low crystalline stability) can explain the low T_k values of gemini TFA.

***n*-Alkylcarboxylate Counterions.** Alkylcarboxylate counterions follow a complex trend in changing their properties as a function of the ion structure, demonstrating a subtle balance among the Coulombic interactions, van der Waals forces, and packing of the organic counterion. The overall mesophase temperature range ΔT ($T_m - T1$) increases first for short- and medium-chain-length anions ($m \leq 6$) (Figure 5). For longer-chain counterions, ΔT decreases as a result of increasing T1 and decreasing T_m. Short-chain *Cm* (C1, C2) behaves like the small anions discussed above whereas the elongation of the chain length leads to another type of packing.

dx.doi.org/10.1021/la304341x | *Langmuir* XXXX, XXX, XXX−XXX

For $2 < m \leq 6$ anions, the decrease in packing due to increasing anion size leads to the competition between Coulombic attraction/repulsion forces and dispersion forces and steric repulsion between the alkyl chain of the counterion and the cation "tail". This balance of forces causes the destabilization of crystalline structures (T1 decreases). For the counterions with $m > 6$, the hydrophobic interaction between long counterion chains and the cation hydrophobic moiety becomes dominant, thus stabilizing the crystalline structure. This causes the increase in T1. The SmA mesophase was observed approximately within the same temperature range (60−80 °C) for short- and medium-chain-length anions whereas this range becomes smaller for the longer-chain anions ($m \geq 8$). For 14-2-14 Palm, the SmA mesophase was not observed, probably because the strong hydrophobic interaction makes the viscous Xb mesophase more favorable than the low-viscosity SmA phase. The melting temperature decreases (from ∼160 to ∼120 °C) for a medium chain length ($2 < m \leq 6$) and then remains similar for a longer chain length, demonstrating the subtle balance among Coulombic interactions, packing stability, and van der Waals forces.

The T_k values of gemini alkylcarboxylates also follows a nonmonotonous trend (Figure 3) with a minimum whereas the hydrophobicity of the alkylcarboxylate shows a uniform increase with chain length (Figure 2). This again confirms that the interplay of the three processes shown in Figure 7 (dissociation, hydration, and micellization) is extremely important for the solubilization mechanism. It is also noteworthy that a similar tendency was observed in the gemini-olygopeptide (Asp-Gly_p-Asp) systems.[70] For these systems, the Krafft temperature has a minimum at $p = 2$ glycyl moieties in the olygopeptide compared to the higher T_k values at $p = 0$ and 4. Along with the molecular area at the air−water interface that also showed a maximum at $p = 2$, such results demonstrate that the aggregation is a cooperative process between intercation/interanion repulsion and attractions due to steric, ionic, hydrophobic, and hydrogen bonding interactions.

The cmc of gemini alkylcarboxylate shows a monotonous decrease with the hydrophobicity order of the anions (except for the 14-2-14 form) (Figure 10).[33] However, the micelle

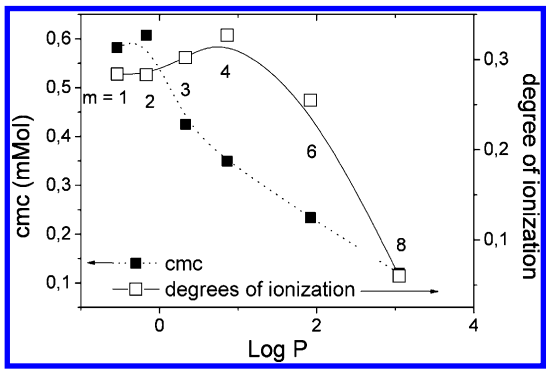

Figure 10. Critical micelle concentrations and 14-2-14 degree of ionization with alkylcarboxylate anions shown as a function of log *P*.

degree of ionization (α) of 14-2-14 alkylcarboxylates again shows a maximum at $m = 3$ to 4, which correlates with the melting temperature (dissociation energy) that goes through the minimum where the weakest binding of a counterion occurs. Short-chain-length counterions are bound mostly electrostatically, and long-chain-length counterions strictly follow their hydrophobicities toward the formation of catanionic micelles with a negligible α. For the medium-chain-length anions, the steric hindrance prevents efficient Coulombic attraction by the headgroup whereas the hydrophobic interaction is too weak to provide hydrophobic binding of the counterion as in catanionic-type surfactants. Strong competition between Coulombic and van der Waals forces and the steric hindrance (packing) of these anions with respect to the headgroups seem to be the main reason for the presence of the break point, for both the thermotropic mesophase and micellar properties in water.

CONCLUSIONS

We have analyzed the role of the nature of the counterion on the overall solubility process using gemini-type cationic surfactants through the comprehensive analysis of different forces. Three steps for the dissolution of an ionic surfactant at the T_k are in play: dissociation, hydration, and micellization. As a first approximation, the T_k values of gemini surfactants are related to the hydrophilicity (ΔG_{hyd}) of the counterions, In general, gemini surfactants with more hydrophilic (smaller ionic radii, higher ΔG_{hyd}) anions demonstrate lower T_k's and higher cmc's. However, a more detailed analysis of the solubilization mechanism indicates that other properties of the compounds are also important, such as the role of the lattice energy (i.e., the stability of the solid states). Indeed, gemini surfactants with smaller counterions have higher melting temperatures and therefore higher lattice energies, and the melting temperature decreases as the ionic radii of the counterions increase. It is also noteworthy that the melting process is complex and includes the formation of LC mesophases. Different types of mesophases have been recognized: crystalline-like smectics, unperturbed nonbirefringent Xa (14-2-14 I, NO_3, and TFA), and viscous birefringent Xb (14-2-14 BR, CL, PH, and all of the alkylcarboxylates). The Xb mesophase is generally followed by less-viscous SmA phases at higher temperature for 14-2-14 with F^-, Cl^-, Br^-, and short-chain alkylcarboxylates, whereas crystalline-like Xa formed by gemini surfactants with more hydrophobic counterions directly transformed to an isotropic phase or underwent degradation. For the mesophase formation temperature, smaller ionic radii resulted in lower transition temperatures.

Among the series of ions, the dihydrophosphate (PH) anion and trifluoroacetate (TFA) show higher or lower T_k's, respectively, which can be expected from their ΔG_{hyd} values. This can be explained by the interplay between the lattice energies of ions (ionic interaction, hydrogene−fluorine low affinity) and the hydration energies of ions.

In summary, the properties of cationic surfactants (solubility, melting, cmc) in the bulk are intimately linked to counterion properties such as the ion size, ion polarizability, ion hydration energy, pK_a, and hydration number. However, the correlation cannot be described by a single parameter and is determined by the subtle interplay between the hydration of counterions and the dissociation energies (stability of crystallinity) of the ion pair.

ASSOCIATED CONTENT

Supporting Information

Crystalline and birefringent phase CR. This material is available free of charge via the Internet at http://pubs.acs.org.

dx.doi.org/10.1021/la304341x | *Langmuir* XXXX, XXX, XXX−XXX

AUTHOR INFORMATION

Corresponding Author

*E-mail: r.oda@iecb.u-bordeaux.fr.

Notes

The authors declare no competing financial interest.

Y.K. is on a leave of absence from Litvinenko Institute, National Academy of Sciences of Ukraine 70, R. Luxemburg Str., 83114 Donetsk, Ukraine.

ACKNOWLEDGMENTS

The Ph.D. theses of S.M. and D.D. were funded by the French Ministry of Education and CNRS, respectively. Y.K. thanks CNRS for financial support to conduct the collaborative projects. We thank E. Ibarboure and S. Lecommandoux of LCPO for their help with DSC measurements. R.O. thanks J. Lacour (U. Geneva) for an inspiring discussion on the term counterions (as he has developed in detail in his feature article in *Chem. Commun.* **2009**, 7073−7089) and L. Cuccia (U. Concordia) for his help in improving the manuscript. We also thank Oleksandr Savsunenko for his help with the images.

REFERENCES

(1) Hofmeister, F. On the Understanding of the Effect of Salts. Second Report. On Regularities in the Precipitating Effect of Salts and Their Relationship to Their Physiological Behavior. *Naunyn-Schmiedebergs Arch. Exp. Pathol. Parmakol. (Leipzig)* **1888**, *24*, 247−260.

(2) Finet, S.; Skouri-Panet, F.; Casselyn, M.; Bonnete, F.; Tardieu, A. The Hofmeister Effect As Seen by SAXS in Protein Solutions. *Curr. Opin. Colloid Interface Sci.* **2004**, *9*, 112−116.

(3) Vogel, R. Influence of Salts on Rhodopsin Photoproduct Equilibria and Protein Stability. *Curr. Opin. Colloid Interface Sci.* **2004**, *9*, 133−138.

(4) Bauduin, P.; Renoncourt, A.; Touraud, D.; Kunz, W.; Ninham, B. W. Hofmeister Effect on Enzymatic Catalysis and Colloidal Structures. *Curr. Opin. Colloid Interface Sci.* **2004**, *9*, 43−47.

(5) dos Santos, A. P.; Levin, Y. Ions at the Water−Oil Interface: Interfacial Tension of Electrolyte Solutions. *Langmuir* **2011**, *28*, 1304−1308.

(6) Baer, M. D.; Mundy, C. J. Toward an Understanding of the Specific Ion Effect Using Density Functional Theory. *J. Phys. Chem. Lett.* **2011**, *2*, 1088−1093.

(7) Kunz, W. Specific ion effects in colloidal and biological systems. *Curr. Opin. Colloid Interface Sci.* **2010**, *15*, 34−39.

(8) Tobias, D. J.; Hemminger, J. C. Getting Specific About Specific Ion Effects. *Science* **2008**, *319*, 1197−1198.

(9) Vrbka, L.; Lund, M.; Kalcher, I.; Dzubiella, J.; Netz, R. R.; Kunz, W. Ion-Specific Thermodynamics of Multicomponent Electrolytes: A Hybrid HNC/MD Approach. *J. Chem. Phys.* **2009**, *131*, 154109.

(10) Jungwirth, P. Spiers Memorial Lecture Ions at Aqueous Interfaces. *Faraday Discuss.* **2009**, *141*, 9−30.

(11) Ishiyama, T.; Morita, A. Molecular Dynamics Study of Gas-Liquid Aqueous Sodium Halide Interfaces. I. Flexible and Polarizable Molecular Modeling and Interfacial Properties. *J. Phys. Chem. C* **2007**, *111*, 721−737.

(12) Kunz, W.; Lo Nostro, P.; Ninham, B. W. The Present State of Affairs with Hofmeister Effects. *Curr. Opin. Colloid Interface Sci.* **2004**, *9*, 1−18.

(13) Bostrom, M.; Williams, D. R. M.; Ninham, B. W. Ion Specificity of Micelles Explained by Ionic Dispersion Forces. *Langmuir* **2002**, *18*, 6010−6014.

(14) Ninham, B. W.; Yaminsky, V. Ion Binding and Ion Specificity: The Hofmeister Effect and Onsager and Lifshitz Theories. *Langmuir* **1997**, *13*, 2097−2108.

(15) Sun, L.; Li, X.; Hede, T.; Tu, Y.; Leck, C.; Ågren, H. Molecular Dynamics Simulations of the Surface Tension and Structure of Salt Solutions and Clusters. *J. Phys. Chem. B* **2012**, *116*, 3198−3204.

(16) Anacker, E. W.; Ghose, H. M. Counterions and Micelle Size. II. Light Scattering by Solutions of Cetylpyridinium Salts. *J. Am. Chem. Soc.* **1968**, *90*, 3161−3166.

(17) Anacker, E. W.; Underwood, A. L. Organic Counterions and Micellar Parameters. *n*-Alkyl Carboxylates. *J. Phys. Chem.* **1981**, *85*, 2463−2466.

(18) Romsted, L. S. Do Amphiphile Aggregate Morphologies and Interfacial Compositions Depend Primarily on Interfacial Hydration and Ion Specific Interactions? The Evidence from Chemical Trapping. *Langmuir* **2007**, *23*, 414−424.

(19) Koelsch, P.; Motschmann, H. Varying the Counterions at a Charged Interface. *Langmuir* **2005**, *21*, 3436−3442.

(20) Lindman, B. Physico-Chemical Properties of Surfactants. In *Handbook of Applied Surface and Colloid Chemistry*; Holmberg, K., Shah, D. O., Schwuger, M. J., Eds.; Wiley: Chichester, U.K., 2002; Vol. *1*, pp 421−444.

(21) Robb, I. D.; Smith, R. Nuclear Spin-Lattice Relaxation Times of Akali Metal Counterions at Micellar Interfaces. *J. Chem. Soc., Faraday Trans. 1* **1974**, *70*, 287−292.

(22) Rosen, M. J. *Surfactants and Interfacial Phenomena*, 3rd ed.; John Wiley & Sons: New York, 2004; p 464.

(23) Zana, R. Ionization of Cationic Micelles: Effect of the Detergent Structure. *J. Colloid Interface Sci.* **1980**, *78*, 330−337.

(24) Myers, D. *Surfactant Science and Technology*, 3rd ed.; John Wiley & Sons: Hoboken, NJ, 2006; p 380.

(25) Cassidy, M. A.; Warr, G. G. Steric and Counterion Effects on Cationic Surfactant Self-Assembly into Micelles and Liquid Crystals. *Aust. J. Chem.* **2003**, *56*, 1065−1070.

(26) Patrick, H. N.; Warr, G. G.; Manne, S.; Aksay, I. A. Surface Micellization Patterns of Quaternary Ammonium Surfactants on Mica. *Langmuir* **1999**, *15*, 1685−1692.

(27) Nemoto, N.; Kuwahara, M. Dynamic Light Scattering of STAB/NASAL Long Threadlike Micelles in the Semidilute Regime: Applicability of the Dynamic Scaling Law. *Langmuir* **1993**, *9*, 419−423.

(28) Totten, G. E.; Goddard, E. D.; Matteson, G. H.; Wanchisen, M. L. Counterion Effects on the Aqueous Solution Cisocity of Cationic Surfactants. *J. Am. Oil Chem. Soc.* **1986**, *63*, 1586−1589.

(29) Abezgauz, L.; Kuperkar, K.; Hassan, P. A.; Ramon, O.; Bahadur, P.; Danino, D. Effect of Hofmeister Anions on Micellization and Micellar Growth of the Surfactant Cetylpyridinium Chloride. *J. Colloid Interface Sci.* **2010**, *342*, 83−92.

(30) Zemb, T.; Belloni, L.; Dubois, M.; Aroti, A.; Leontidis, E. Can We Use Area Per Surfactant As a Quantitative Test Model of Specific Ion Effects? *Curr. Opin. Colloid Interface Sci.* **2004**, *9*, 74−80.

(31) Gurau, M. C.; Lim, S. M.; Castellana, E. T.; Albertorio, F.; Kataoka, S.; Cremer, P. S. On the Mechanism of the Hofmeister Effect. *J. Am. Chem. Soc.* **2004**, *126*, 10522−10523.

(32) Lima, E. R. A.; Bostrom, M.; Biscaia, E. C.; Tavares, F. W.; Kunz, W. Ion Specific Forces between Charged Self-Assembled Monolayers Explained by Modified DLVO Theory. *Colloids Surf., A* **2009**, *346*, 11−15.

(33) Manet, S.; Karpichev, Y.; Bassani, D.; Kiagus-Ahmad, R.; Oda, R. Counteranion Effect on Micellization of Cationic Gemini Surfactants 14-2-14: Hofmeister and Other Counterions. *Langmuir* **2010**, *26*, 10645−10656.

(34) Bunton, C. A.; Robinson, L.; Schaak, J.; Stam, M. F. Catalysis of Nucleophilic Substitutions by Micelles of Dicationic Detergents. *J. Org. Chem.* **1971**, *36*, 2346−2350.

(35) Danino, D.; Talmon, Y.; Zana, R. Alkanediyl-α,ω-bis-(dimethylalkylammonium bromide) Surfactants (Dimeric Surfactants). 5. Aggregation and Microstructure Aqueous Solutions. *Langmuir* **1995**, *11*, 1448−1456.

(36) Zana, R.; Xia, J. *Gemini Surfactants: Synthesis, Interfacial and Solution-Phase Behavior, and Applications*; Marcel Dekker: New York, 2004; Vol. *117*, p 331.

(37) Oda, R.; Laguerre, M.; Huc, I.; Desbat, B. Molecular Organization of Gemini Surfactants in Cylindrical Micelles: An Infrared Dichroism Spectroscopy and Molecular Dynamics Study. *Langmuir* **2002**, *18*, 9659−9667.
(38) Menger, F. M.; Elrington, A. R. Organic Reactivity in Microemulsion Systems. *J. Am. Chem. Soc.* **1991**, *113*, 9621−9624.
(39) Menger, F. M.; Keiper, J. S. Gemini Surfactants. *Angew. Chem., Int. Ed.* **2000**, *39*, 1906−1920.
(40) Jiang, N.; Li, P.; Wang, Y.; Wang, J.; Yan, H.; Thomas, R. K. Micellization of Cationic Gemini Surfactants with Various Counterions and Their Interaction with DNA in Aqueous Solution. *J. Phys. Chem. B* **2004**, *108*, 15385−15391.
(41) Jiang, N.; Li, P.; Wang, Y.; Wang, J.; Yan, H.; Thomas, R. K. Aggregation Behavior of Hexadecyltrimethylammonium Surfactants with Various Counterions in Aqueous Solution. *J. Colloid Interface Sci.* **2005**, *286*, 755−760.
(42) Aime, C.; Manet, S.; Satoh, T.; Ihara, H.; Park, K.-P.; Godde, F.; Oda, R. Self-Assembly of Nucleoamphiphiles: Investigation Nucleosides Effect and the Mechanism of Micrometric Helix Formation. *Langmuir* **2007**, *23*, 12875−12885.
(43) Brizard, A.; Ahmad, R. K.; Oda, R. Control of Nano-micrometric Twist and Helical Ribbon Formation with Gemini-Oligoalanine via Interpeptidic Beta-Sheet Structure Formation. *Chem. Commun.* **2007**, *22*, 2275−2277.
(44) Brizard, A.; Aime, C.; Labrot, T.; Huc, I.; Berthier, D.; Artzner, F.; Desbat, B.; Oda, R. Counterion, Temperature, And Time Modulation of Nanometric Chiral Ribbons from Gemini-Tartrate Amphiphiles. *J. Am. Chem. Soc.* **2007**, *129*, 3754−3762.
(45) Oda, R.; Huc, I.; Candau, S. J. Gemini Surfactants As New, Low Molecular Weight Gelators of Organic Solvents and Water. *Angew. Chem., Int. Ed.* **1998**, *37*, 2689−2691.
(46) Oda, R.; Huc, I.; Schmutz, M.; Candau, S. J.; MacKintosh, F. C. Tuning Bilayer Twist Using Chiral Counterions. *Nature* **1999**, *399*, 566−569.
(47) Wang, Y. J.; Desbat, B.; Manet, S.; Aime, C.; Labrot, T.; Oda, R. Aggregation Behaviors of Gemini Nucleotide at the Air-Water Interface and in Solutions Induced by Adenine-Uracil Interaction. *J. Colloid Interface Sci.* **2005**, *283*, 555−564.
(48) Wang, Y. J.; Marques, E. F. Mesophase Formation and Thermal Behavior of Catanionic Mixtures of Gemini Surfactants with Sodium Alkylsulfates. *J. Therm. Anal. Calorim.* **2010**, *100*, 501−508.
(49) Zhou, T. H.; Zhao, J. X. Synthesis and Thermotropic Liquid Crystalline Properties of Heterogemini Surfactants Containing a Quaternary Ammonium and a Hydroxyl Group. *J. Colloid Interface Sci.* **2009**, *331*, 476−483.
(50) Zhou, T. H.; Zhao, J. X. Synthesis and Thermotropic Liquid Crystalline Properties of Zwitterionic Gemini Surfactants Containing a Quaternary Ammonium and a Sulfate Group. *J. Colloid Interface Sci.* **2009**, *338*, 156−162.
(51) Gulaboski, R.; Riedl, K.; Scholz, F. Standard Gibbs Energies of Transfer of Halogenate and Pseudohalogenate Ions, Halogen Substituted Acetates, And Cycloalkyl Carboxylate Anions at the Water|Nitrobenzene Interface. *Phys. Chem. Chem. Phys.* **2003**, *5*, 1284−1289.
(52) Aime, C.; Plet, B.; Manet, S.; Schmitter, J. M.; Huc, I.; Oda, R.; Sauers, R. R.; Romsted, L. S. Competing Gas-Phase Substitution and Elimination Reactions of Gemini Surfactants with Anionic Counterions by Mass Spectrometry. Density Functional Theory Correlations with Their Bolaform Halide Salt Models. *J. Phys. Chem. B* **2008**, *112*, 14435−14445.
(53) Ubbelohde, A. R. *The Molten State of Matter: Melting and Crystal Structure*; Wiley: Chichester, U.K., 1978.
(54) Demus, D.; Goodby, J. W.; Gray, G. W.; Spiess, H. W.; Vill, V.*Handbook of Liquid Crystals*; Wiley-VCH Verlag GmbH: Weinheim, Germany, 2008 (set).
(55) Paleos, C. M. Thermotropic Liquid-Cristals Derived from Amphiphilic Mesogens. *Mol. Cryst. Liq. Cryst. Sci. Technol., Sect. A* **1994**, *243*, 159−183.
(56) Dierking, I. *Textures of Liquid Crystals*. Wiley-VCH: Weinheim, Germany, 2003.
(57) Alami, E.; Levy, H.; Zana, R.; Weber, P.; Skoulios, A. A New Smectic Mesophase with 2-Dimensional Tetragonal Symmetry from Dialkyldimethylammonium Bromide. *Liq. Cryst.* **1993**, *13*, 201−212.
(58) Axenov, K. V.; Laschat, S. Thermotropic Ionic Liquid Crystals. *Materials* **2011**, *4*, 206−259.
(59) Goossens, K.; Lava, K.; Nockemann, P.; Van Hecke, K.; Van Meervelt, L.; Driesen, K.; Gorller-Walrand, C.; Binnemans, K.; Cardinaels, T. Pyrrolidinium Ionic Liquid Crystals. *Chem.—Eur. J.* **2009**, *15*, 656−674.
(60) Nikokavoura, A.; Tsiourvas, D.; Arkas, M.; Sideratou, Z.; Paleos, C. M. Thermotropic Liquid Crystalline Behaviour of Piperazinium and Homopiperazinium Alkylsulphates. *Liq. Cryst.* **2002**, *29*, 1547−1553.
(61) Ohta, K.; Sugiyama, T.; Nogami, T. A Smectic T Phase of 1,4-Dialkyl-1,4-diazoniabicyclo 2.2.2 Octane Dibromides. *J. Mater. Chem.* **2000**, *10*, 613−616.
(62) Binnemans, K. Ionic Liquid Crystals. *Chem. Rev.* **2005**, *105*, 4148−4204.
(63) Luo, S. C.; Sun, S. W.; Deorukhkar, A. R.; Lu, J. T.; Bhattacharyya, A.; Lin, I. J. B. Ionic Liquids and Ionic Liquid Crystals of Vinyl Functionalized Imidazolium Salts. *J. Mater. Chem.* **2011**, *21*, 1866−1873.
(64) Ster, D.; Baumeister, U.; Chao, J. L.; Tschierske, C.; Israel, G. Synthesis and Mesophase Behaviour of Ionic Liquid Crystals. *J. Mater. Chem.* **2007**, *17*, 3393−3400.
(65) Manku, G. S. *Theoretical Principles of Inorganic Chemistry*; Tata McGraw-Hill: New Delhi, 1982.
(66) Steed, J. W.; Atwood, J. L. *Supramolecular Chemistry*; Wiley: New York, 2000.
(67) Slater, J. C. Theory of the Transition in KH_2PO_4. *J. Chem. Phys.* **1941**, *9*, 16−33.
(68) Ubbelohde, A. R.; Woodward, I. Structure and Thermal Properties Associated with Some Hydrogen Bonds in Crystals IV. Isotope Effects in Some Acid Phosphates. *Proc. R. Soc. London, Ser. A* **1942**, *179*, 0399−0407.
(69) Zamponi, F.; Rothhardt, P.; Stingl, J.; Woerner, M.; Elsaesser, T. Ultrafast Large-Amplitude Relocation of Electronic Charge in Ionic Crystals. *Proc. Natl. Acad. Sci. U.S.A.* **2012**, *109*, 5207−5212.
(70) Brizard, A.; Dolain, C.; Huc, I.; Oda, R. Asp-Gly Based Peptides Confined at the Surface of Cationic Gemini Surfactant Aggregates. *Langmuir* **2006**, *22*, 3591−3600.